RSC Advances

ROYAL SOCIETY OF CHEMISTRY

www.rsc.org/advances

Journal Name

ARTICLE

Comparison of the oxidative pyrolysis behaviors of black liquor solids, alkali lignin and enzymatic hydrolysis/mild acidolysis lignin

Received 00th January 20xx,
Accepted 00th January 20xx

DOI: 10.1039/x0xx00000x

www.rsc.org/

Hao Cheng,[a] Shubin Wu*[a] and Xiaohong Li[a]

The oxidative pyrolysis of black liquor solid (BLS), alkali lignin (AL), and enzymatic hydrolysis/ mild acidolysis lignin (EMAL) from the same cunninghamia lanceolata was studied by pyrolysis coupled with gas chromatograph-mass spectrometer (Py-GC-MS) at 600 °C in air atmosphere. A closed tubular reactor was used to study the oxidative pyrolysis of the three samples. The effect of reaction time on the product was investigated. It was found that oxygen dramatically promoted the decomposition of lignin. Guaiacol and 4-methyl-guaiacol were the top two products in BLS and AL, while coniferyl aldehydel and 4-vinyl-guaiacol yielded the top two in EMAL. The yield of noncondensable gas increased with the reaction time, while the yield of phenolic compounds decreased quickly if the reaction time was more than 60 seconds in AL and EMAL.

Introduction

Lignin, nature's dominant aromatic polymer, is found in most terrestrial plants in the approximate range of 15 to 40% day weight and provides structural integrity.[1] It is the most recalcitrant of the three components of lignocellulosic biomass (cellulose, hemicellulose and lignin).[2] It is predominantly obtained from cooking liquors produced in pulping processes.[3] The advent of new cellulosic biorefineries however, will introduce an excess supply of different, nonsulfonated, native and transgenically modified lignin into the process streams.[1] Therefore, the efficient utilization of lignin resources is necessary for both the paper-making industry and in cellulosic bio-refinery.

Fast pyrolysis, which is known as a promising process to convert pretreated biomass to bio-oil, is affected by the biomass types and reaction conditions.[4] It is an effective method to convert biomass into high value gaseous, liquid and solid fuels.[5] Since this biomass fast pyrolysis is an endothermic process,[6] and therefore requires an external energy input, much attention has been paid to reducing the energy consumption during the pyrolysis process. Oxidative pyrolysis, greatly simplifies the reactor design to reduce the energy input and improves the conversion rate of biomass, [7-13] as shown in these studies. On the other hand, carefully controlled oxygen concentration in partial oxidative pyrolysis would be beneficial to the decomposition of biomass and reduce the content of oligomers or pyrolytic lignin in bio-oil.[11]

Oxidative pyrolysis behavior varies in different materials. For example, the sugar yield of red oak is improved at the oxygen content of 4.2 vol%,[10] sulfur of solid waste can be significantly reduced under oxidative environment,[14] and the heat value in the oxidative pyrolysis of pine wood is much higher than that of inert condition.[5] BLS and AL, which represent a part of the residue from the soda pulping process, are burned to supply energy and recover pulping chemicals in the operation of paper mills,[15] while the preparation of EMAL is similar to the cellulosic bio-refinery. The different oxidative pyrolysis behaviours of them exhibit important effect on the full utilization of them.

In this study, BLS, AL, and EMAL are isolated from the same cunninghamia lanceolata. Simultaneous thermal analysis of them in air atmosphere from ambient temperature up to 800 °C is conducted using a TG–DSC/DTA apparatus. The oxidative pyrolysis of them are investigate in the Py-GC-MS and self-designed pyrolysis reactor at 600 °C with air atmosphere. The research focused on the different pyrolysis characteristics of them.

Materials and methods

Sample Preparation

The black liquor sourcing from cunninghamia lanceolata came from a pulping mill in Guangdong province. The black liquor was dried in an oven at 105 °C for 24h, and then dried in a vacuum drying oven at 50 °C for 72h to prepare the black liquor solids (BLS). A pure alkali lignin sample was then separated from the black liquor by acid precipitation with H_2SO_4 (10%, w/w) to pH 2. The acid precipitated solids were then filtered from the solution, washed thoroughly with distilled water, and freeze dried. The EMAL lignin was isolated using the enzymatic/mild acidolysis method.[16] The ash content of BLS, AL and EMAL was 45.36%, 1.69%, and 0.73%, respectively.

Fourier Transform Infrared Spectroscopy (FTIR)

[a] Address here. State Key Laboratory of Pulp and Paper Engineering, South China University of Technology, Guangzhou, Guangdong 510640, PR China
* Corresponding author: Email: shubinwu@scut.edu.cn
Telephone/Fax: +86-20-22236808
Electronic Supplementary Information (ESI) available: [details of any supplementary information available should be included here]. See DOI: 10.1039/x0xx00000x

Infrared analysis of the three samples was conducted utilizing a Nicolet IS50 fourier transform infrared spectrometer (FTIR, Thermo Fisher Scientific, USA) with a DTGS detector. The sample blending potashbromide (sample: KBr = 1:100, w/w, KBr, spectrographic grade) was pressed using a type Tianjin HF-2 press machine. Spectra were obtained in the range of 400 to 4000cm^{-1} with a resolution of 4cm^{-1}, and 64 scans were obtained for each sample.

Simultaneous Thermal Analysis (STA)

STA refers to the simultaneous measurement of TG and differential scanning calorimetry (DSC) on the same sample in the same instrument.[17] The thermal analyses were performed using a Netzsch STA 449F3 Jupiter Simultaneous Thermal Analyzer (TG–DSC/DTA Apparatus). In each experiment, approximately 15 mg of the sample was used, and tests performed from ambient temperature up to 800 °C with a constant heating rate of 10 °C/min. The total air flow during all measurements was 60 ml/min.

Pyrolysis coupled with Gas Chromatograph-Mass Spectrometer (Py-GC-MS)

The Py-GC-MS systems were performed using a CDS5200 pyroprobe (CDS, USA). The pyroprobe was operated in the trapping mode, with reactant gas of air and a tenax trap. Approximately 0.1 mg of sample was dried at 80 °C for 5s, then it was pyrolyzed at 600 °C at a heating rate of 10 °C/ms for 10s. The pyrolysate was collected in a trap, which was precooled at -50 °C by liquid nitrogen. Then the trap was desorbed at 300 °C for 4min to the gas chromatography-mass spectroscopy (GC-MS) via a heated transfer line at 300 °C. The GC-MS analysis of the pyrolysis products was conducted with an Agilent 7890A gas chromatography equipped with a 5975C mass selective detector (Agilent Technologies, USA) with an ion source of electron impact (EI) at 70 eV. The flow rate of the carrier gas was 45 mL/min with a split ratio of 40:1 and the injection temperature was 300 °C. The pyrolysis products were then separated in an Agilent DB-5ms capillary column (30 m × 0.25 mm × 0.25 μm). The temperature programming was as follows: the GC oven was kept at 50 °C for 1 min and programmed to 300 °C at an increment of 10 °C/min, holding for 5 min. The mass range m/z 33-550 was scanned. Identification of the pyrolysis compounds was achieved by comparing their mass fragment with the NIST 08 mass spectral library.

Construction and Operation of Pyrolysis Reactor

Fig. 1 shows the schematic diagram and the operation of the newly designed pyrolysis reactor. This reactor was comprised of a pyrolysis unit based on a vertical tubular furnace, of which the temperature was controlled by a PID controller(EC5530, Ohkura) and a movable pyrolysis tube (7) made of quartz (200 mm long×35mm wide×6 mm o.d.×4 mm i.d.).It was set inside of an outer tube (300 mm long×45 mm i.d.). The most obvious advantage of this pyrolysis reactor was the measurement of heating and the complete collection of the liquid products. Also, the reaction could stop quickly to reduce the recombination of the liquid products.

About 150 mg of each sample was introduced into the U-quartz tube. The vacuum union tee and the U-quartz tube were connected by a cap nut, then the pyrolysis unit was purged with air for 10min under the flow at 50 mL/min. The valve (3) was then closed the keep an airtight system. The above steps were finished outside of the vertical tubular furnace (8). After the furnace had stabilized at the desired temperature of 600 °C, fast pyrolysis was conducted by inserting the pyrolysis units into the furnace at a fixed position and holding for 1-3 min. The thermocouple (4) showed the pyrolysis temperature was reached to 600 °C in 50 seconds. After the pyrolysis, the U-quartz tube was immediately cooled with cold deionized water for 1min. (The temperature of deionized water was about 10 °C, and the temperature of the U-quartz tube dropped to 200 °C in about 5 seconds, and dropped to 25°C after 1min). Then the valve (3) was opened to release the pyrolysis volatiles by purging N_2 (99.995%, 30 mL/min) for 10 min. The non-condensable gases were collected in a gasbag (10) and analyzed offline. The U-quartz tube was extracted with methanol (5 mL×3) and then diluted with methanol to 25.00 mL. The methanol-soluble fractions were analyzed with GC-MS.

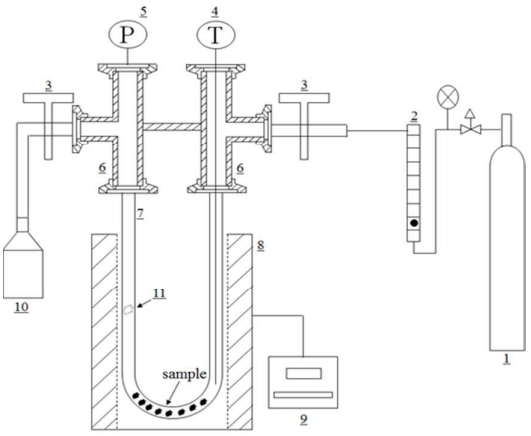

Fig. 1. Schematic diagram and operation of pyrolysis unit with movable U-quartz tube reactor. (1) Cylinder gas, (2) Nitrogen flow meter, (3) Valve, (4) Thermocouple, (5) Piezometer, (6) Vacuum union tee, (7) U-quartz tube, (8) Vertical tubular furnace, (9) Temperature controller, (10) Gas collecting unit, (11) Silica wool.

RESULTS AND DISCUSSION

FTIR Analysis

Spectra from the three samples in question are shown in Fig. 2. AL and EMAL spectra share nearly the uniform peaks, whereas BLS exhibits greater variation in peak position and intensities, as well as fewer peaks. Since BLS contains sodium phenolate structure, the aromatic C-C stretch is focused to 1598 cm^{-1}, C-O stretch of Ar-OH

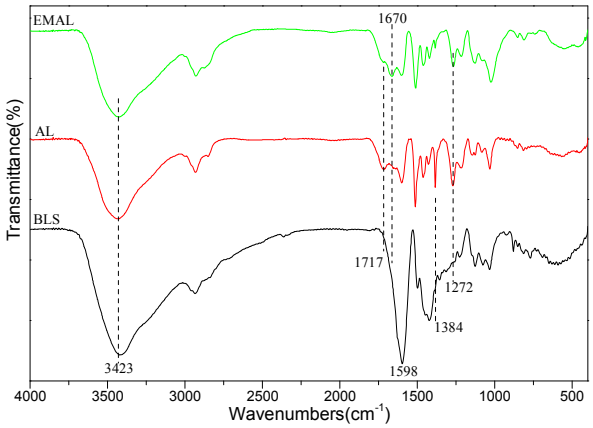

(1272 cm^{-1}) and in-plane O-H bend (1384 cm^{-1})[18] have vanished. In

comparison to BLS, the spectra from AL and EMAL show

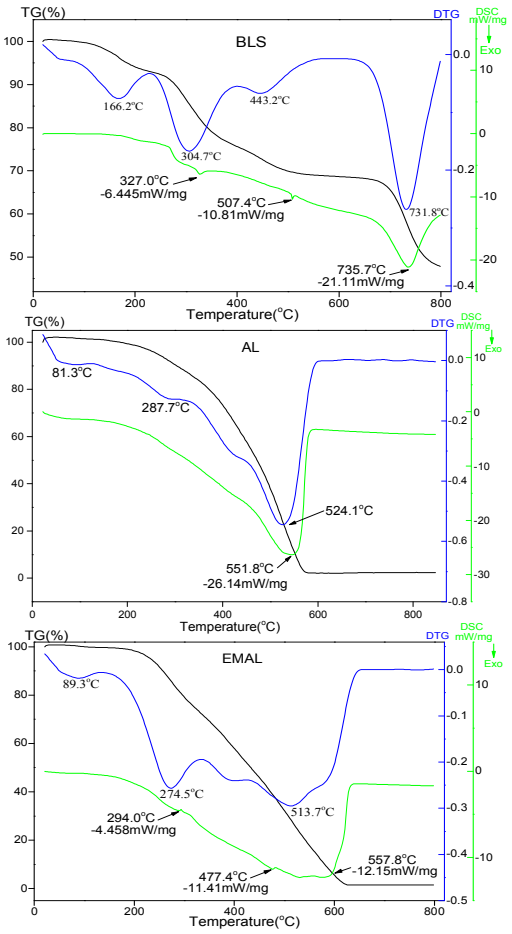

significantly greater peaks at 1670 and 1717 cm^{-1}, indicating a greater presence of carbonyl groups. Overall, the FTIR spectra illustrate greater functional groups content of AL and EMAL.

Fig. 2. FTIR spectra of BLS, AL and EMAL

Simultaneous Thermal Analysis

Fig. 3. Temperature-dependent mass change (TG), rate of mass change (DTG), heating flow rate (DSC) of BLS, AL and EMAL.

It can be seen from Fig. 3 that there are three main stages in the DTG curves of AL and EMAL, which can be divided into dehydration, oxidation pyrolysis and char oxidation.[5, 7] The obvious peak at 731.8 °C in BLS, represents the decomposition of metal salt in it.[15] The DTG curve of AL appears to be more uniform and identical in distribution. This observation results from the breakage of labile functional groups in the preparation process of AL.

Even with an air-dry material, a small mass loss is observed in the temperature range of 60 to 100 °C, which is connected to the evaporation of water.[5, 15, 19] In addition to moisture, the BLS contains a peak at 166.2 °C, which is water released out by the crack of aliphatic hydroxyl groups in the lateral chains. [15] In the conducted measurements, only a little mass loss was observed in the water evaporation zone.

The oxidation pyrolysis step occurs in the range of 180 to 320 °C, which is lower than the inert atmosphere.[20, 21] The mass loss of BLS, AL, and EMAL in this range is 10.59%, 7.90%, and 14.91%, respectively. The most interesting observation is the small endothermic peak at around 294 °C in the DSC curve of EMAL, which result from the melting and crosslinking of its macromolecular structure.

The char oxidation stage starts from around 320 °C to 600 °C. The mass loss of this step is 14.49%, 85.87%, 73.90% of BLS, AL, and EMAL, respectively. Based on the DSC, curves have a big exothermic peak in this step, so we conclude that the main heat comes from the char oxidation in the whole reaction process. The residual parts at the final temperature are found to be 47.95%, 2.44% and 1.35% for BLS, AL and EMAL, respectively. It is close to the ash content and it can be concluded that the organic part are nearly burned out at this condition. While the residual yield of AL and EMAL are much higher with a heating rate of 40 °C/min.[22]

Flash Oxidative Pyrolysis of BLS, AL and EMAL on Py-GC-MS

The advantage of pyrolysis coupled with the GC-MS technique, is a high heating rate which can be available to prevent the upcoming

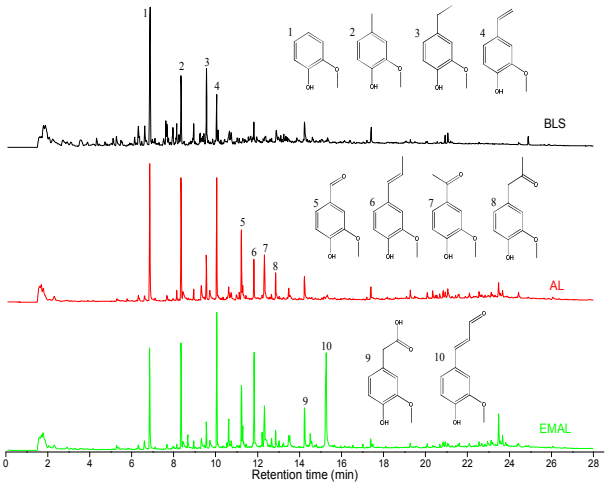

second reaction.[23] According to the DTG curves, the pyrolysis temperature was set at 600 °C to ensure each sample decomposed completely. The obtained total ion-current spectrograms of Py-GC-MS from BLS, AL and EMAL at 600 °C are exhibited in Fig. 4 and the analysis of pyrolysis products are showed in Table S1 (see the ESI*).

Fig. 4. Total ion-current spectrograms of BLS, AL and EMAL with Py-GC-MS

Pyrolytic products of BLS, AL and EMAL detected by Py-GC-MS were shown in Table S1 (see the ESI*). It can be seen that the relative contents of each compound changes with different samples. Guaiacol and 4-methyl-guaiacol yields the top two in BLS and AL, while coniferyl aldehydel and 4-vinylphenol are the top two products in EMAL. The difference is probably due to the chemical structure and molecular weight of samples.[16] EMAL has lower breakage of the lignin structure units, so the C_{10} and C_9 phenolic compounds make up the majority products of EMAL. The apparent difference is the peak at 15.3 min in EMAL, which is linked to coniferyl aldehyde. Overall, the Py-GC-MS results provide more valuable structural characterization than any other method.

Oxidative Pyrolysis of BLS, AL and EMAL in a Closed Reactor

Analyzed by GC-TCD, the non-condensable gas products from oxidative pyrolysis of the three samples are similar, mainly including CO_2, CO, CH_4, C_2H_6 and a very small amount of H_2 and C_2H_4. A typical profile of each gas yield (wt. % of sample) varied with time increasing is showed in Fig. 5.

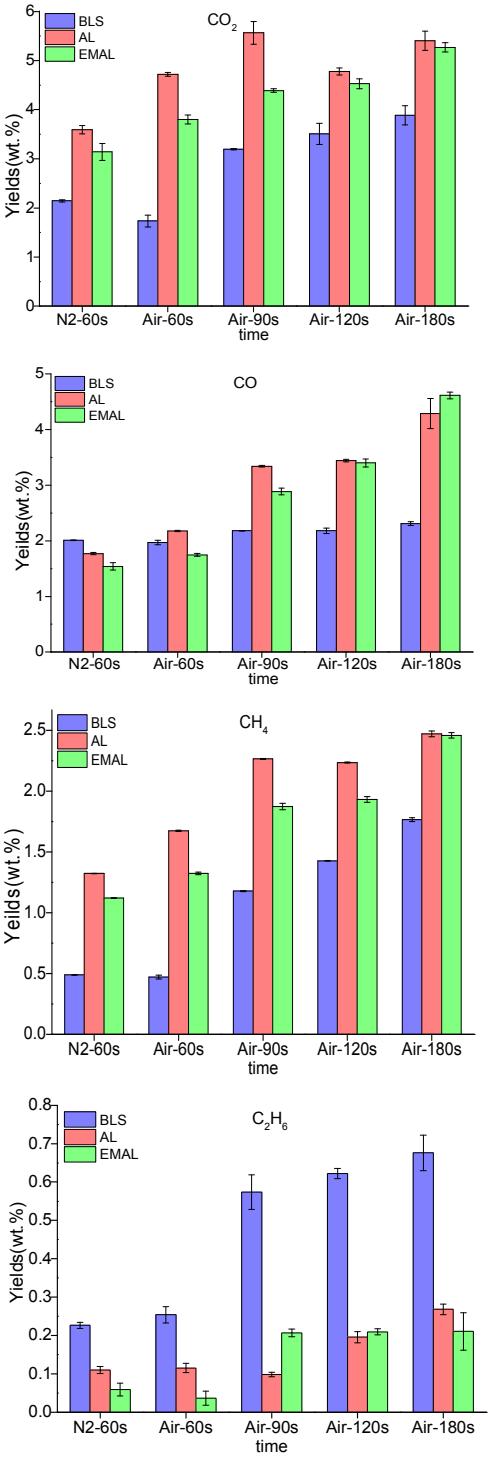

Fig. 5. Gas yields as a function of time

Compared with BLS, the CO_2 content in AL and EMAL is higher, which is consistent with the observation in FTIR that AL and EMAL have more carbonyl groups. Owing to the reaction between phenolic hydroxyl and ortho methoxy,[24-26] the CH_4 content in AL and EMAL is higher than BLS, while CO concentration stays almost the same in BLS. Since the breakage of $ArO\text{-}CH_3$ has a lower energy barrier than $Ar\text{-}OCH_3$,[27] and the phenolic hydroxyl is broken in BLS, the conversion of C_2H_6, which is from the combination of two methyl radicals, is higher in BLS than the other two samples.

Fig. 6 shows the results of the qualitative examination of several selected compounds of liquid products by GC-MS. It is obviously found that the effect of air oxidation pyrolysis in 3 minutes to the main liquid products of BLS is little. There is a peak of vanillin at air-120 s in AL, while vanillin content in EMAL drops with the reaction time, which may due to the chemical structure difference of AL and EMAL. The results in Fig.6 indicate that the residence time of the oxidative pyrolysis should be controlled in 60s to best utilization of the three kinds of lignin.

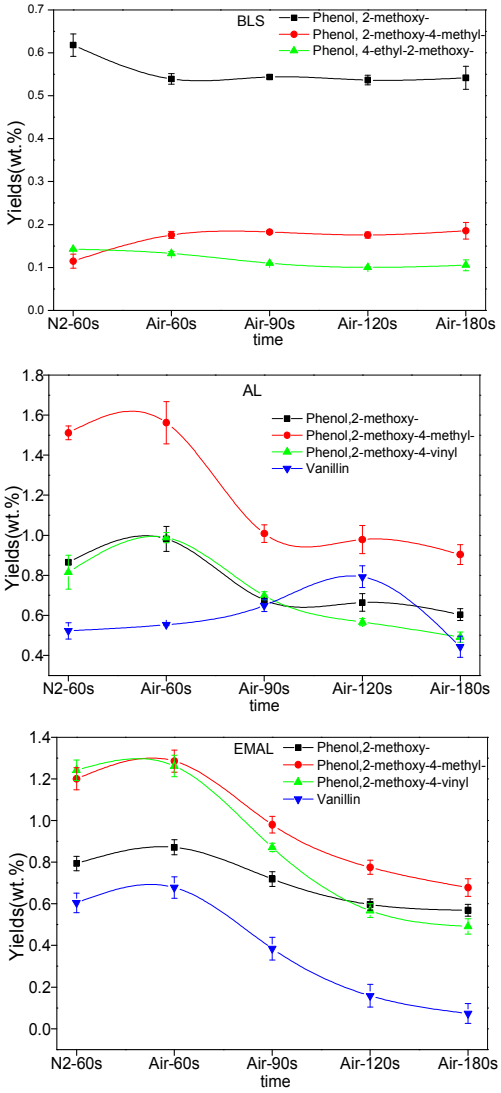

Fig. 6. The effect of time on the yield of selected compounds in BLS, AL, and EMAL

Conclusions

The oxidative pyrolysis process of AL and EMAL could be divided into three steps: dehydration, oxidation pyrolysis and char oxidation. The biggest exothermic peak of AL and EMAL was around 550 °C, while BLS peaked at about 735 °C. This result could direct the energy utilization of them.

The oxidative pyrolysis of the samples mainly were phenolic compounds. Wherein, C_9 and C_{10} phenolic compounds were the major tar products of EMAL, while C_8 and C_9 phenolic compounds were found in BLS and AL. The yield of C_2H_6 in BLS was higher than AL and EMAL, while the content of CH_4 in AL and EMAL was more than BLS. The residence time of should be controlled in 60s at 600 °C to best utilization of the three kinds lignin.

Acknowledgements

This work was supported by the National Basic Research Program of China (973 Program, 2013CB228101).

Notes and references

1 A. J. Ragauskas, G. T. Beckham, M. J. Biddy, R. Chandra, F. Chen, M. F. Davis, B. H. Davison, R. A. Dixon, P. Gilna, M. Keller, P. Langan, A. K. Naskar, J. N. Saddler, T. J. Tschaplinski, G. A. Tuskan and C. E. Wyman, *Science*, 2014, **344**, 1246843.
2 A. Rahimi, A. Ulbrich, J. J. Coon and S. S. Stahl, *Nature*, 2014, **515**, 249-252.
3 X. M. Huang, T. I. Koranyi, M. D. Boot and E. J. M. Hensen, *Chemsuschem*, 2014, **7**, 2276-2288.
4 M. Asadieraghi, W. M. Ashri Wan Daud and H. F. Abbas, *RSC Adv.*, 2015, **5**, 22234-22255.
5 Y. Su, Y. H. Luo, W. G. Wu, Y. L. Zhang and S. H. Zhao, *J Anal Appl Pyrol*, 2012, **98**, 137-143.
6 F. He, W. Yi and X. Bai, *Energy Conversion and Management*, 2006, **47**, 2461-2469.
7 E. Daouk, L. Van de Steene, F. Paviet and S. Salvador, *Chemical Engineering Science*, 2015, **126**, 608-615.
8 M. Amutio, G. Lopez, R. Aguado, J. Bilbao and M. Olazar, *Energy & Fuels*, 2012, **26**, 1353-1362.
9 D. A. E. Butt, *J Anal Appl Pyrol*, 2006, **76**, 38-47.
10 K. H. Kim, R. C. Brown and X. Bai, *Fuel*, 2014, **130**, 135-141.
11 D. Li, C. Briens and F. Berruti, *Biomass and Bioenergy*, 2015, **76**, 96-107.
12 H. Zhang, R. Xiao, D. Wang, J. Cho, G. He, S. Shao and J. Zhang, *Chemical Engineering Journal*, 2012, **181-182**, 685-693.
13 H. Y. Zhang, R. Xiao, Q. W. Pan, Q. L. Song and H. Huang, *Chemical Engineering & Technology*, 2009, **32**, 27-37.
14 M. Y. Wey, S. C. Huang and C. L. Shi, *Fuel*, 1997, **76**, 115-121.
15 D. L. Guo, S. B. Wu, B. Liu, X. L. Yin and Q. Yang, *Appl Energ*, 2012, **95**, 22-30.
16 S.Wu and D. S. Argyropoulos, *Journal of Pulp and Paper Science*, 2003, **29**, 235-240.
17 A. Schindler, G. Neumann, A. Rager, E. Füglein, J. Blumm and T. Denner, *Journal of Thermal Analysis and Calorimetry*, 2013, **113**, 1091-1102.
18 H. Nadji, P. N. Diouf, A. Benaboura, Y. Bedard, B. Riedl and T. Stevanovic, *Bioresource technology*, 2009, **100**, 3585-3592.
19 M. A. Bazelatto Zanoni, H. Massard and M. Ferreira Martins, *Combustion and Flame*, 2012, **159**, 3224-3234.
20 J. B. Li, S. B. Wu and X. H. Li, *Bioresources*, 2013, **8**, 5120-5132.
21 H. Zhou, Y. Long, A. Meng, S. Chen, Q. Li and Y. Zhang, *RSC Adv.*, 2015, **5**, 26509-26516.
22 H. Haykiri-Acma, S. Yaman and S. Kucukbayrak, *Energy Conversion and Management*, 2011, **52**, 746-751.
23 R. Lou, S. Wu, G. Lv and Q. Yang, *Appl Energ*, 2012, **90**, 46-50.
24 M. Asmadi, H. Kawamoto and S. Saka, *J Anal Appl Pyrol*, 2011, **92**, 88-98.
25 M. Asmadi, H. Kawamoto and S. Saka, *Holzforschung*, 2012, **66**.
26 C. Liu, Y. Zhang and X. Huang, *Fuel Processing Technology*, 2014, **123**, 159-165.
27 R. Alen, E. Kuoppala and P. Oesch, *J Anal Appl Pyrol*, 1996, **36**, 137-148.